Development Report:

Garbage Detection Using YOLOv3 in Nakanoshima Challenge

Jingwei Xue, Zehao Li, Masahito Fukuda, Tomokazu Takahashi, Masato Suzuki, Yasushi Mae, Yasuhiko Arai, and Seiji Aoyagi

Kansai University
3-3-35 Yamate-cho, Suita, Osaka 564-8680, Japan
E-mail: {k465705, k762378, k765977, t.taka, m.suzuki, mae, arai, aoyagi}@kansai-u.ac.jp
[Received July 7, 2020; accepted October 20, 2020]

Object detectors using deep learning are currently used in various situations, including robot demonstration experiments, owing to their high accuracy. However, there are some problems in the creation of training data, such as the fact that a lot of labor is required for human annotations, and the method of providing training data needs to be carefully considered because the recognition accuracy decreases due to environmental changes such as lighting. In the Nakanoshima Challenge, an autonomous mobile robot competition, it is challenging to detect three types of garbage with red labels. In this study, we developed a garbage detector by semi-automating the annotation process through detection of labels using colors and by preparing training data by changing the lighting conditions in three ways depending on the brightness. We evaluated the recognition accuracy on the university campus and addressed the challenge of using the discriminator in the competition. In this paper, we report these results.

Keywords: deep learning, object detector

1. Introduction

Object detection has recently become an important elemental technology in a wide range of fields such as automated driving, autonomous robots, and home robots. Object detection is used to indicate the location of an object in the input image. Deep learning methods have recently attracted attention to achieve high accuracy in object detection [1–6].

Deep learning object detectors require a large amount of training data and training time to achieve high accuracy. Here, training data is created by collecting image data and annotating an object (i.e., specifying the position of an object in the image). The accuracy of the detector obtained through machine learning, including deep learning, is greatly influenced by the quality of the training data used [4]. In addition, the accuracy of an object detector is likely to deteriorate in outdoor environments where the visibility of the object changes with brightness. Autonomous mobile robot competitions, such as the Tsukuba Challenge, provide a good opportunity to address such issues for the development of object detectors. For the purpose to participate in the Tsukuba Challenge, we participated in the Nakanoshima Challenge held in Osaka last year, and worked on the semi-automation of the annotation of training data and the creation of a dataset with different lighting conditions (brightness). In this paper, we report the results of the evaluation of recognition accuracy on the university campus and the results of the object recognition challenge using the detector in the competition.

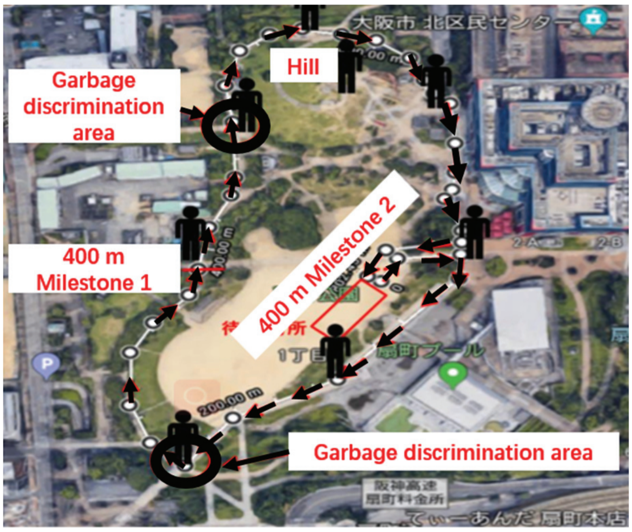

Fig. 1. Map of course and garbage detection area.

2. Garbage Discrimination Challenge in Nakanoshima Challenge

2.1. Garbage Detection Location

The Nakanoshima Challenge was held in September and December 2019 in Nakanoshima Park and Ogimachi Park in Osaka City, respectively. We tackled the task of detecting garbage in the latter competition. The garbage detection task was conducted at two locations in the course, as shown in **Fig. 1**. There was always a staff member in the same position as the garbage.

(a) Garbage label

(b) Bottle, convenience store bento, can of garbage (convenience store bento is abbreviated simply as bento in the following of this article.)

(c) Flag in Nakanoshima Challenge

(d) Garbage shown to the camera

Fig. 2. Garbage with label and staff showing it to the camera.

2.2. Types of Garbage

Three types of garbage were detected: 500 mL PET bottle, 350 mL can, and convenience store bento (hereinafter simply called "bento" meaning lunch box). All the trash was wrapped using a red band with the Nakanoshima Challenge 2019 logo. **Fig. 2** shows photographs of the logo and garbage.

2.3. Implementation Procedure for Garbage Detection Task

The implementation procedure for garbage detection task is as follows.

(1) The robot stops within a 3-meter radius around the staff holding the garbage.

(2) If (1) is fulfilled, the staff holding the garbage will present the garbage to the camera mounted on the robot. The robot recognizes this and transmits the results by some means of communication.

The stopping method in (1) is not specified. Therefore, the following measures are possible:

- The robot recognizes the flags near the staff and stops within a certain radius from the staff. The photograph of the flag is shown in **Fig. 2(c)**.
- The robot recognizes the safety vest of the staff and stops within a certain radius from the staff.
- A waypoint is placed in the vicinity of the point where the garbage is presented on the map. The staff who presents the garbage is always in the position shown in the two garbage discrimination areas in **Fig. 1**. The robot moves while performing localization and stops at waypoint. (We chose this stopping method.)

The means of communicating the results are not specified in (2). Therefore, the following measures are possible:

- The results are transmitted in audio.
- The results are displayed on a PC screen. (We chose this method.)
- The results are shown using lamps (LEDs, etc.) corresponding to the three types of garbage.

Three pieces of garbage were presented, one for each of the three types described in Section 2.2. These pieces were presented in random order, and the results must be presented within 20 s per result. A recognition retry was allowed for 20 s. If the result could not be shown within 20 s, it was judged to be a failure and the next garbage was presented.

3. Garbage Detection Method

3.1. Employing YOLOv3 as Garbage Recognition Method

We adopted YOLOv3 as the object detection method based on deep learning [7]. We needed to specify the type of object in a training image by enclosing it with a square (called a bounding box), which is called the annotation operation. It is often done manually, and it is labor intensive to obtain a large amount of training data.

In addition, it is necessary to obtain training data under various lighting conditions to improve the recognition accuracy in a changeable environment such as outdoors.

3.2. Definition of Brightness

Three types of lighting conditions (full, normal, and insufficient) were defined numerically as the brightness of the outside environment. The method used to determine the brightness is described below.

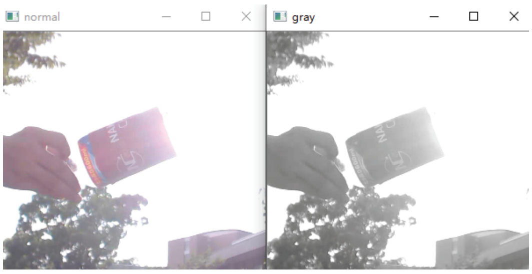

Fig. 3. Normal picture (left) and grayscale picture (right).

Table 1. Light intensity range defined in this experiment.

Kind of daylight	Range for averaged gray value		
	Min.	Max.	Illuminance
Full (Sunny A.M.)	170	240	25,000–100,000 lx
Normal (Cloudy P.M.)	90	170	2,000–25,000 lx
Insufficient (Cloudy A.M.)	25	90	300–2,000 lx

As shown in **Fig. 3**, OpenCV is used to convert RGB images into grayscale images. The average of the grayscale is obtained using the following equation [8, 9]:

$$\text{Average grayscale} = \frac{\text{Sum of all grayscale values of the entire image}}{\text{Total number of pixels of the entire image}}.$$

Table 1 shows the relationship between the average grayscale value and the illuminance measured using an illuminometer at the time the image was taken. When the mean value of the grayscale is 170, the illuminance value is 25,000 lx, and when it is 240, the illuminance value is 100,000 lx. According to [10, 11, a, b], the illuminance values in this range correspond to the brightness in the morning on a clear day. Similarly, the illuminance value in range of 2,000–25,000 lx corresponds to the brightness in the afternoon on a cloudy day, and the illuminance value in range of 300–2,000 lx corresponds to the brightness in the morning on a cloudy day. In this study, we call these brightness values full, normal, and insufficient, respectively, as shown in **Table 1**.

3.3. Environment to Create Dataset

To create a dataset, the camera is mounted on the robot, and the images are collected while the robot is moving. This allows us to match the image quality and visibility created by the camera's installation conditions (height and tilt) to the actual conditions for object detection. The camera is a web camera (C920r by Logitech, 1920×1080 pixel resolution). The appearance of the mobile robot and the installation conditions of the camera are shown in **Fig. 4**. The angle of the camera is 15° upward. The images are collected from the movies and by cutting out still images frame by frame from them.

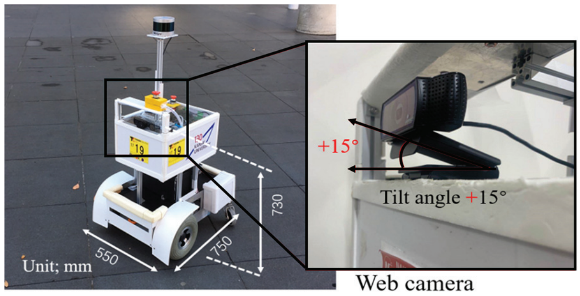

Fig. 4. Outline of mobile robot "KUARO" developed by Kansai University and web camera installed on it.

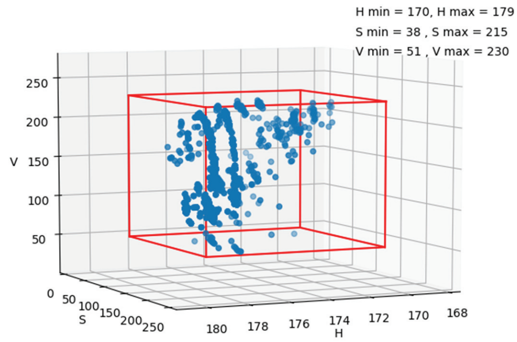

Fig. 5. HSV scatter plot.

3.4. Method to Create Dataset

Manual annotation is a major burden in the creation of datasets. To solve this problem, we created a program to perform semi-automatic annotation tasks using the OpenCV library and the red labels attached to the garbage shown in **Fig. 2** [c, d].

The flow of the program is as follows.

1. We convert the characteristic color of an object from RGB to HSV and obtain the value of HSV [12, 13], taking into account that red in HSV is more likely to be detected than RGB regardless of the brightness. The range of the red HSV feature color is specified, as shown in **Fig. 5**, and the image is binarized on the basis of whether it is in or out of this range.
   Here, **Fig. 5** shows that 100 images are randomly selected for full, normal, and insufficient lightning conditions. The pixels in the red labels in the images were randomly selected, and their HSV values were plotted. The range of the red color was defined as $170 \leq$ (H-value) ≤ 179, $38 \leq$ (S-value) ≤ 215, and $51 \leq$ (V-value) ≤ 230 based on the data.
2. A region with a large HSV feature color area is determined (labeling process). The outline of the region is shown in green in **Fig. 6 (1)**.
3. A rectangle circumscribed by the contour is obtained. The rectangle is shown in pink in **Fig. 6 (2)**.
4. The height of the rectangle in **Fig. 6 (2)** is expanded twice in the case of a PET bottle and bento, and

(1) The largest red color area is extracted. Its contour is colored in green in this figure.

(2) An external rectangle of the contour is obtained, which is colored in pink.

(3) In the cases of bottle and bento, the height of the rectangle is doubled. In the case of can, the height is increased by 1.2 times. The rectangle colored in blue is obtained.

(4) Through the coordinates of four vertices of the blue rectangle, the last rectangle colored in red is obtained.

Fig. 6. The procedure of annotation of can, bento and bottle.

the height of the rectangle in **Fig. 6 (2)** is expanded by 1.2 times in the case of a can, to obtain the blue rectangle in **Fig. 6 (3)**. These magnification rates are based on the width of the labels (100 mm) and the actual longitudinal size of the objects (210 mm for a bento and PET bottle, and 125 mm for a can).

5. The final rectangle is obtained from the coordinates of the four vertices of the rectangle in **Fig. 6 (3)**. The rectangle is shown in red in **Fig. 6 (4)**.

6. The final rectangle is a bounding box with YOLO training data. The final rectangle is used as a bounding box, and its location is saved using the still image.

7. The steps 1–6 are repeated to create a dataset.

We studied three types of garbage: PET bottle, bento, and can, as described in Section 2.2. The above annotation program automatically determines the position of the bounding box, but the three types of objects are categorized by humans in advance. In addition, if the image is out of focus, it is judged by humans and excluded from the training image in advance. Furthermore, the positions of the automatically calculated bounding boxes are checked by humans, and those that are obviously in the wrong position are excluded from the training data (there was such a case under the insufficient condition, and about 20 images were removed manually when 10,500 images of training data were generated). Thus, although the annotation process is programmed, it requires human assistance, and therefore, it is semi-automated rather than fully automated. The accuracy rate of the annotations is 100%

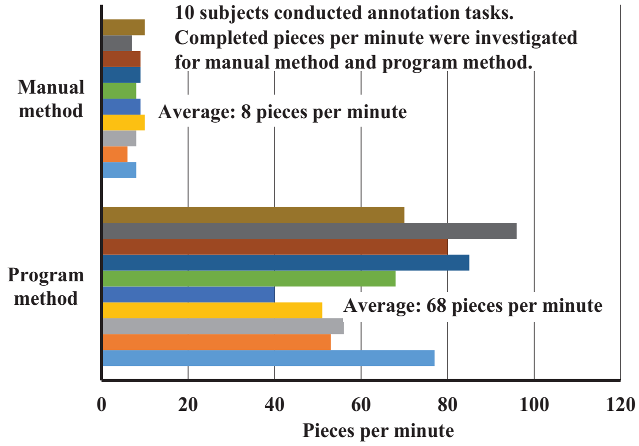

Fig. 7. Annotation task is drastically speeded up by using program method instead of manual method.

because human judgment ultimately intervenes.

To investigate the effectiveness of the semi-automated program for annotation, 20 subjects (all volunteers in their 20s) were recruited. A total of 10 subjects performed the annotation task completely manually, and the remaining 10 performed the task semi-automatically using the program and only confirming the results. **Fig. 7** shows the number of images for which the annotations can be performed in a minute. On average, 8 images could be processed manually, and 68 could be processed semi-automatically using the program, thereby improving the work efficiency by approximately 8 times.

Data were collected under three different lightning conditions, as shown in **Table 1**. Finally, 10,000 training images of each object were collected. The total number of dataset images was 30,000. The breakdown of 10,000 images of each object was 3,500 full images, 3,000 normal images, and 3,500 insufficient images to equally include the images with different brightness values. An example of the dataset that we created is shown in **Fig. 8**.

4. Garbage Detection Experiment in Actual Environment

4.1. Specifications of Computer

The specifications of the computer used in this study were 16 GB memory, Nvidia GeForce GTX 1080 graphics card, and Ubuntu 16.04.2 operating system. The dataset of 30,000 images, described in Section 3.4, was divided into a training set of 27,000 images and a test dataset of 3,000 images. The test datasets were chosen to ensure that the brightness and the number of data were equal for each type of garbage. The test datasets were used to check the performance of the detector during training.

The weights of the neural network were updated using the momentum method [14, 15], according to the following equations:

$$V \leftarrow \alpha V - \eta \frac{\partial L}{\partial W}, \quad \ldots \ldots \ldots \quad (1)$$

$$W \leftarrow W + V. \quad \ldots \ldots \ldots \quad (2)$$

where V is the momentum (the amount of weight update), α is the momentum coefficient, η is the learning rate, L is the loss (residual), and W is the weight.

Table 2 lists the parameters used for training. Batch size is the number of images used per update, and weight decay is the decay coefficient used to prevent the increase in weight due to overtraining [16, 17].

4.2. Consideration of the Number of Trainings

The vertical axis on the left side of **Fig. 9** is the loss, and the horizontal axis is the number of training cycles. The convergence curve becomes flat after approximately 2,500 training sessions.

We empirically set the recognition threshold [18, 19] for object recognition to 0.7 (if the obtained value is greater than or equal to this threshold, it is judged as a specified object). We used two indices to evaluate the performance of the detector: the false rejection rate (FRR), the probability of not recognizing the target object in the image, and the false acceptance rate (FAR), the probability of misidentifying the target object as another object.

Figure 9 shows the relationship between the mean values of FRR and FAR for the test dataset (in units of [%] on the right vertical axis) and the number of trainings (horizontal axis). The FRR decreases and the FAR increases when the number of trainings is below 50,000 (the two are reciprocal [20]). However, when the number exceeds 50,000, the values do not change. Considering this, we stopped training and saved the weights when the number of trainings reached 50,000. At this moment, the loss value is 0.1.

4.3. Results of Cross Validation

To measure the generalization performance of the trained detector, we performed a 5-fold cross-validation test. A total of 30,000 images of the dataset are divided into five blocks. Each block contains 6,000 images, and the number of images for each type of trash and its brightness is equal. As shown in **Fig. 10**, one of the five blocks is used as the verification data and the others as training data. The FRR and FAR for the cross-validation are shown in **Figs. 11** and **12**, respectively. These results confirmed that the trained detector had good generalization performance because there was no significant difference between the five recognition results.

4.4. Contribution to the Recognition Rate of Datasets with Varying Brightness

We examined the contribution of full (bright) and insufficient (dark) datasets to discrimination performance. As shown in **Fig. 13**, a total of 9,000 images of training data (3,000 images × 3 kinds of garbage) are selected from the

Fig. 8. Annotation of three kinds of garbage in different daylight conditions. 15 images are displayed for each kind of garbage among 10,000.

Table 2. Several important parameters in machine learning.

Momentum α	0.9
Weight decay	0.0005
Batch size	16
Learning rate η	0.001

full training data (a total of 10,500 images; 3,500 images of the garbage per object) explained in Section 3.4, and these are used as the training dataset. Using this dataset, we trained 50,000 times to obtain the detector.

A total of 1,000 out of the remaining 1,500 images of full are selected to evenly distribute the number of data for each object type. 1,000 images are selected from each of the training data of normal images (normal brightness, 3,000 images for each object, 9,000 images in total) and the training data of insufficient images (3,500 images per object, 10,500 images in total) to make the number of image data for each object type equal. These are combined to form a 3,000-image verification dataset. This breakdown is as follows: three lightning conditions × (333 images of PET bottles + 334 images of bentos + 333 images of cans). We denote the discrimination experiment using this detector and test dataset as Test 1.

In the same way, as shown in **Fig. 13**, we train and construct the detector using 9,000 images of the insufficient training data, and construct a set of 3,000 test dataset images with all brightnesses. We call this experiment Test 2. The experimental results are shown in **Figs. 14** and **15**,

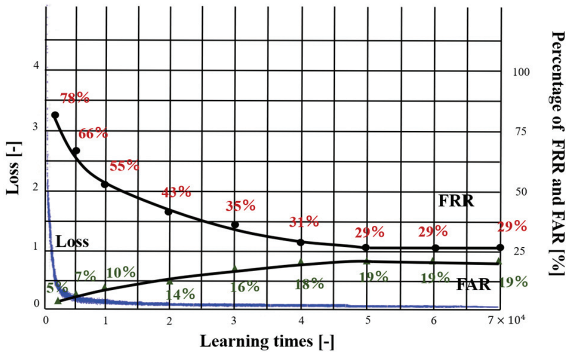

Fig. 9. Loss function convergence curve.

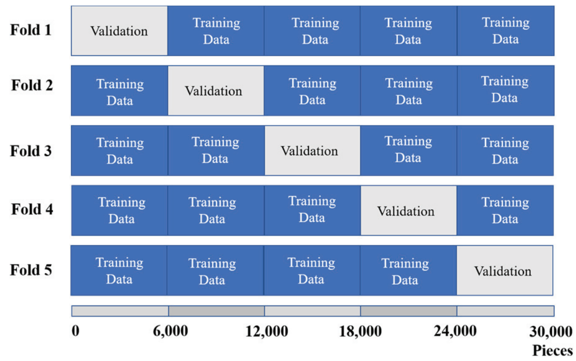

Fig. 10. Dataset for 5-fold cross-validation of which object and lightning varied equally.

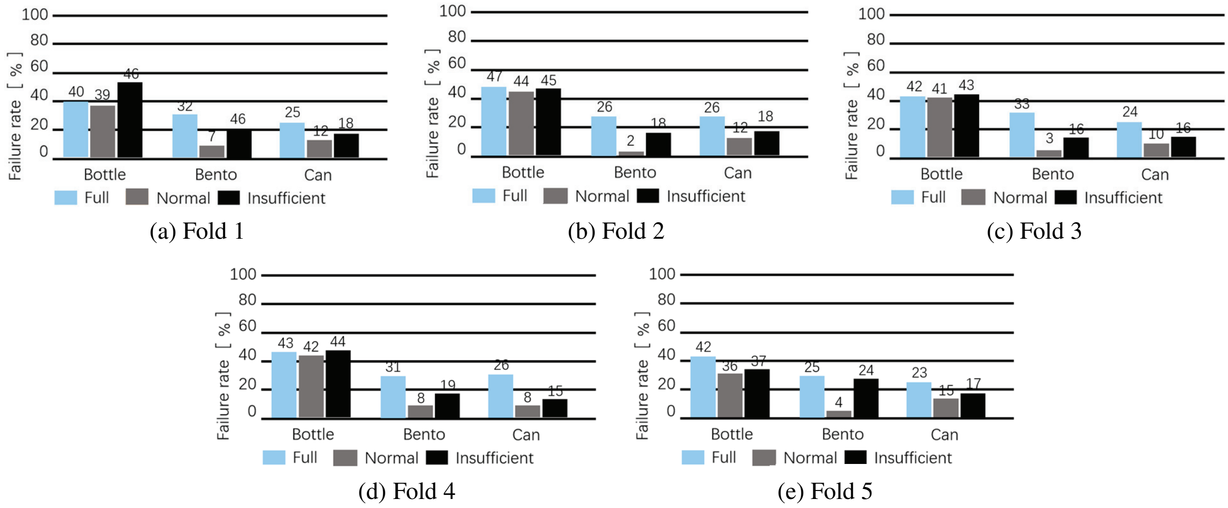

Fig. 11. False rejection rate (FRR) of 5-fold cross validation.

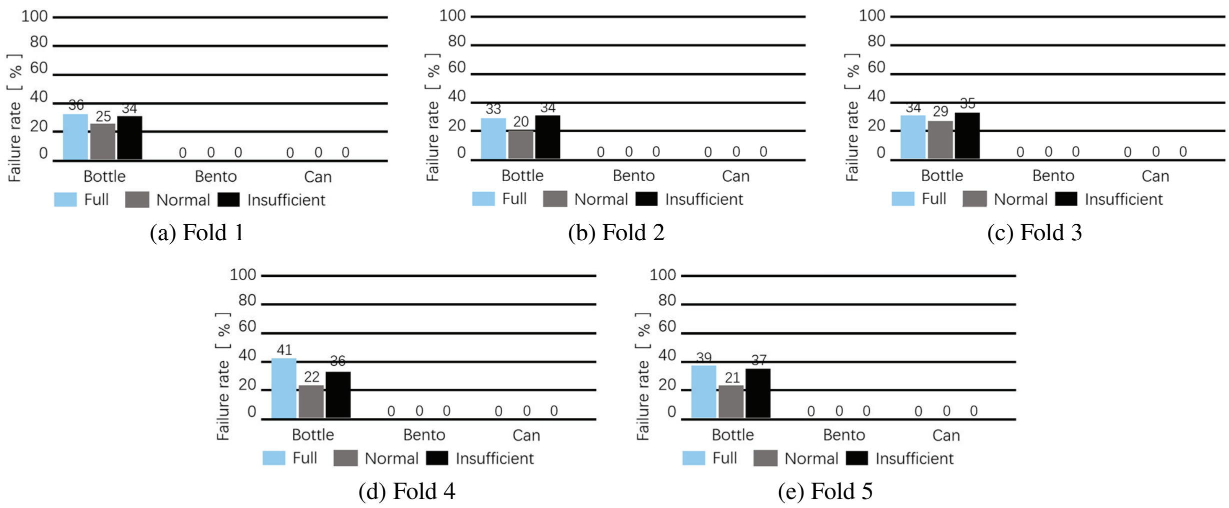

Fig. 12. False acceptance rate (FAR) of 5-fold cross validation.

where in Test 1 the FRR is low under the full condition (high recognition accuracy) and high in the normal and insufficient conditions (low recognition accuracy). Similarly, in Test 2, the FRR is low for insufficient, which is used in training, and high in other cases. This shows that training the detector at a limited brightness degrades the accuracy at other brightness levels. In other words, we found that training the detector at various brightness levels is effective in improving accuracy. This has been shown experimentally in [21, 22].

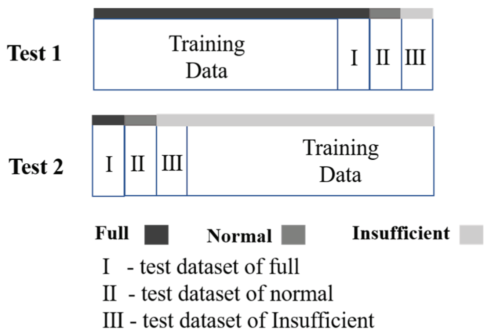

Fig. 13. Dataset for illuminance influence test.

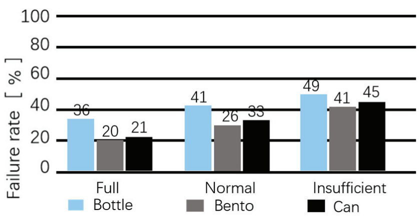

Fig. 14. FRR for object recognition based on training with only full dataset (Test 1).

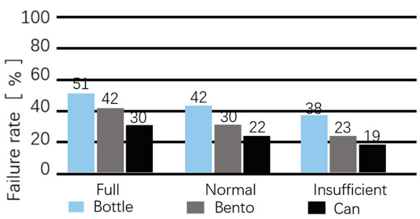

Fig. 15. FRR for object recognition based on training with only insufficient dataset (Test 2).

4.5. Comprehensive Test Results for Unknown Image

We tested the trained detector. In addition to the dataset, we used a test dataset on the campus for the three types of garbage under the three lightning conditions shown in **Table 1**. We prepared 340 test datasets for each condition, which are approximately the same number of datasets as the test dataset used in Section 4.1. In other words, a total of 3,060 images were prepared from 340 images × three lightning conditions × three garbage types. That is, we prepared the test dataset to make the number of data for each brightness and each type of garbage equal.

The FRR results are shown in **Fig. 16**, and the FAR results are shown in **Fig. 17**. It can be seen from **Fig. 16** that all objects can be easily recognized under the normal daylight condition. An example of a successful test is shown in **Fig. 18**. Under the insufficient daylight or full daylight condition, the objects were not recognized well, as shown in **Fig. 19**.

Figure 17 shows that there is no misrecognition of cans and bentos as other objects. The recognition rate for cans

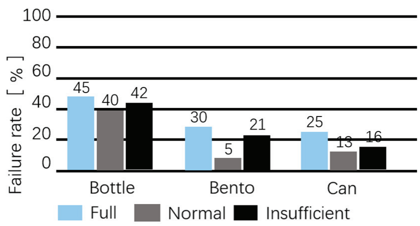

Fig. 16. False rejection rate (FRR).

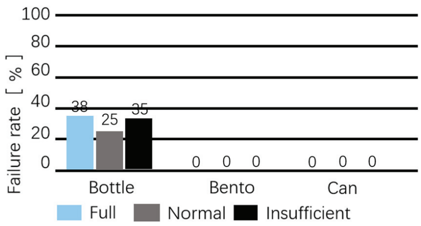

Fig. 17. False acceptance rate (FAR).

Fig. 18. The successfully detected examples of the recognition system with YOLOv3 in normal daylight condition.

Fig. 19. Unrecognized pictures.

and bentos is higher than that for PET bottles in **Fig. 16**. On the other hand, the FAR for PET bottles is high, and there are many cases of misrecognition of PET bottles as cans, as shown in **Fig. 20**. The PET bottles were not misrecognized as bentos and were all misrecognized as cans. It can be seen from **Fig. 20** that the two main reasons for this are that PET bottles and cans are similar when only the label part is viewed, and that the part of the bot-

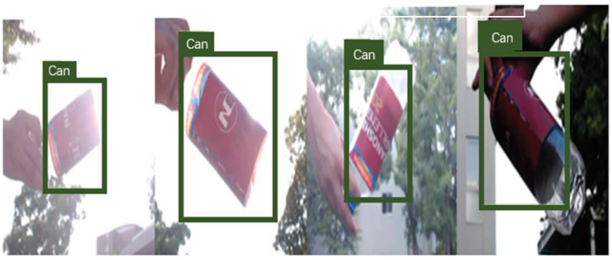

Fig. 20. The bottle is mistakenly identified as a can.

(a) Successful recognition results in “Nakanoshima Challenge” robot competition

(b) Grasp method the same as (a) in training data set

Fig. 21. Successful recognition results in “Nakanoshima Challenge” robot competition.

tle other than the label is transparent and difficult to see. **Fig. 17** shows that the effect of brightness moderates the misrecognition of PET bottles to some extent, but even in normal daylight, where the FAR is the lowest, the FAR is 25%. Therefore, we believe that the change in visibility due to the change in the brightness is not the main cause.

4.6. Results on the Day of Competition

The example of the success of the recognition results for the garbage detection task on the day of the Nakanoshima Challenge is shown in **Fig. 21(a)**. The way to hold the garbage when it is presented in the competition is also implemented in the training data collection. The image of this training is shown in **Fig. 21(b)**.

The problem of garbage recognition was solved. However, the misrecognition of PET bottles as cans, as described in Section 4.5, was also observed on the day of the competition. This situation is shown in **Fig. 22**.

5. Conclusions

We worked on detecting garbage in the Nakanoshima Challenge robot competition. The training data were collected in consideration of the outdoor lighting environment. We semi-automated the annotation process of the training data using red labels attached to the garbage. We evaluated the outdoor accuracy of the object detector based on the above methods. Under normal daylight, the FRR and FAR were 40% and 25% for PET bottles, 5% and 0% for bentos, and 13% and 0% for cans, respectively. The results for both FRR and FAR were unsatisfactory for PET bottles.

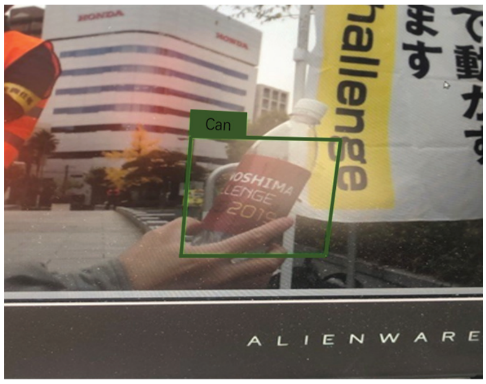

Fig. 22. Misidentification of PET bottle as can in “Nakanoshima Challenge” robot competition.

In this study, we collected the same amount of data for each type of brightness and used them for training. In the future, we will perform training by increasing the brightness data that have yielded unsatisfactory results in the present study, and we will add pre-processing to mitigate the difference in brightness, instead of absorbing it using the object detector. In addition to our efforts to cope with the brightness, we will also work on the recognition of transparent objects.

Acknowledgements

This study was financially supported by the Kansai University Educational Research Enhancement Fund in 2020 under the title of “Real World Service Innovation through the AI Robot Challenge.”

References:

[1] J. Redmon, S. Divvala, R. Girshick, and A. Farhadi, “You only look once: Unified, Real-Time Object Detection,” 2016 IEEE Conf. on Computer Vision and Pattern Recognition (CVPR), 2016.
[2] D. Erhan, C. Szegedy, A. Toshev, and D. Anguelov, “Scalable object detection using deep neural networks,” 2014 IEEE Conf. on Computer Vision and Pattern Recognition (CVPR), 2014.
[3] K. He, X. Zhang, S. Ren, and J. Sun, “Spatial pyramid pooling in deep convolutional networks for visual recognition,” IEEE Trans. on Pattern Analysis and Machine Intelligence, Vol.37, Issue 9, pp. 1904-1916, 2015.
[4] N. Chavali, H. Agrawal, A. Mahendru, and D. Batra, “Object-Proposal Evaluation Protocol is ‘Gameable’,” 2016 IEEE Conf. on Computer Vision and Pattern Recognition (CVPR), 2016.
[5] C. Szegedy, A. Toshev, and D. Erhan, “Deep neural networks for object detection,” Neural Information Processing Systems (NIPS), Vol.13, No.2, pp. 2553-2561, 2013.
[6] A. R. Pathak, M. Pandey, and S. Rautaray, “Application of Deep Learning for Object Detection,” Procedia Computer Science, Vol.132, pp. 1706-1717, 2018.
[7] J. Redmon and A. Farhadi, “YOLOv3: An Incremental Improvement,” arXiv: 1804.02767, 2018.
[8] K. Tarun and V. Karun, “A Theory Based on Conversion of RGB image to Gray image,” Int. J. of Computer Applications, Vol.7, No.2, pp. 1140-1439, 2010.

[9] C. Saravanan, "Color Image to Grayscale Image Conversion," 2010 Second Int. Conf. on Computer Engineering and Applications, Vol.2, pp. 196-199, 2010.

[10] M. H. Toufiq Imam, J. Gleason, S. Mishra, and M. Oishi, "Estimation of solar heat gain using illumination sensor measurements," Solar Energy, Vol.174, pp. 296-304, 2018.

[11] A. Kaminska and A. Ożadowicz, "Lighting Control Including Daylight and Energy Efficiency Improvements Analysis," Energies, Vol.11, pp. 2166-2184, 2018.

[12] P. Ganesan, V. Rajini, B. S. Sathish, and B. S. Khamar, "HSV Color Space Based Segmentation of Region of Interest in Satellite Images," 2014 Int. Conf. on Control, Instrumentation, Communication and Computational Technologies (ICCICCT), pp. 196-199, 2014.

[13] S. Shailaja and K. K. Ramesh, "Shadow Suppression Using RGB and HSV Color Space in Moving Object Detection," Int. J. of Advanced Computer Science and Applications, Vol.4, No.1, 2013.

[14] B. T. Polyak, "Some methods of speeding up the convergence of iteration methods," USSR Computational Mathematics and Mathematical Physics, Vol.4, pp. 1-17, 1964.

[15] I. Sutskever, J. Martens, G. Dahl, and G. Hinton, "On the importance of initialization and momentum in deep learning," Int. Conf. on Machine Learning, pp. 1139-1147, 2013.

[16] R. M. Zur, Y. Jiang, and L. L. Pesce, "Noise injection for training artificial neural networks: A Comparison with Weight Decay and Early Stopping," Medical Physics, Vol.36, pp. 4810-4818, 2009.

[17] G. Zhang, C. Wang, B. Xu, and R. Grosse, "Three mechanisms of weight decay regularization," Int. Conf. on Learning Representations, 2019.

[18] C. Liu, P. M. Berry, T. Dawson, and R. G. Pearson, "Selecting thresholds of occurrence in the prediction of species distributions," Ecography, Vol.28, No.3, pp. 385-393, 2005.

[19] P. Ren, W. Fang, and S. Djahel, "A Novel YOLO-Based real-time people counting approach," 2017 Int. Smart Cities Conf. (ISC2), pp. 1-2, 2017.

[20] M. Adámek, M. Matýsek, and P. Neumann, "Security of Biometric Systems," Procedia Engineering, Vol.100, pp. 169-176, 2015.

[21] K. Sivaraman and A. Murthy, "Object Recognition under Lighting Variations using Pre-Trained Networks," 2018 IEEE Applied Imagery Pattern Recognition Workshop (AIPR), pp. 1-7, 2018.

[22] N. P. Ramaiah, E. P. Ijjina, and C. K. Mohan, "Illumination invariant face recognition using convolutional neural networks," 2015 IEEE Int. Conf. on Signal Processing, Informatics, Communication and Energy Systems (SPICES), pp. 1-4, 2015.

Supporting Online Materials:

[a] Daylight. https://en.wikipedia.org/wiki/Daylight [Accessed August 12, 2019]

[b] Osaka Science Museum. http://photon.sci-museum.kita.Osaka.jp/publish/text/koyomi.html [Accessed August 12, 2019]

[c] OpenCV. https://opencv.org/ [Accessed August 12, 2019]

[d] OpenCV. https://docs.opencv.org/ [Accessed August 12, 2019]

Name:
Jingwei Xue

Affiliation:
Master Student, Kansai University

Address:
3-3-35 Yamate-cho, Suita, Osaka 564-8680, Japan

Brief Biographical History:

2018 Received B.E. degree in Industrial Engineering from Setsunan University

Name:
Zehao Li

Affiliation:
Research Student, Kansai University

Address:
3-3-35 Yamate-cho, Suita, Osaka 564-8680, Japan

Brief Biographical History:

2018 Received B.E. degree in Mechanical Design, Manufacturing and Automation from Xian University of Architecture and Technology

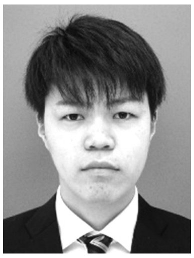

Name:
Masahito Fukuda

Affiliation:
Master Student, Kansai University

Address:
3-3-35 Yamate-cho, Suita, Osaka 564-8680, Japan

Brief Biographical History:

2019 Received B.E. degree in Industrial Engineering, Kansai University

Main Works:

- "Shape Information Recognizer for Object Recognition Using Object Concept," Image Laboratory, Japan Industrial Publishing Co., Vol.31, No.5, pp. 39-45, 2020.

Membership in Academic Societies:

- The Japan Society of Mechanical Engineers (JSME)

Name:
Tomokazu Takahashi

Affiliation:
Associate Professor, Kansai University

Address:
3-3-35 Yamate-cho, Suita, Osaka 564-8680, Japan

Brief Biographical History:

2010 Received Ph.D. degree in the Mechanical Engineering from Tohoku University

2010- Assistant Professor, Mechanical Engineering Department, Kansai University

2015- Associate Professor, Mechanical Engineering Department, Kansai University

Main Works:

- T. Takahashi, S. Kikuchi, M. Suzuki, and S. Aoyagi, "Vacuum Gripper Imitated Octopus Sucker-Effect of Liquid Membrane for Absorption," 2015 IEEE/RSJ Int. Conf. on Intelligent Robots and Systems, Hamburg, Germany, Sept. 28-Oct. 03, pp. 2929-2936, 2015.

Membership in Academic Societies:

- The Institute of Electrical and Electronics Engineers (IEEE)
- The Japan Society of Mechanical Engineers (JSME)

Name:
Masato Suzuki

Affiliation:
Associate Professor, Kansai University

Address:
3-3-35 Yamate-cho, Suita, Osaka 564-8680, Japan

Brief Biographical History:
2007 Received Ph.D. degree in Semiconductor Engineering from Hiroshima University
2009- Assistant Professor, Mechanical Engineering Department, Kansai University
2013- Associate Professor, Mechanical Engineering Department, Kansai University

Membership in Academic Societies:
- The Japan Society of Applied Physics (JSAP)

Name:
Yasushi Mae

Affiliation:
Professor, Faculty of Engineering Science, Kansai University

Address:
3-3-35 Yamate-cho, Suita, Osaka 564-8680, Japan

Brief Biographical History:
1998- Research Associates, Osaka University
2004- Associate Professor, University of Fukui
2007- Associate Professor, Osaka University
2019- Professor, Kansai University

Main Works:
- "Brain Machine Interface System Automation considering User Preferences and Error Perception Feedback," IEEE Trans. on Automation Science and Engineering, Vol.11, Issue 4, pp. 1275-1281, 2014.
- "Object search using object co-occurrence relations derived from web content mining," J. of Intelligent Service Robotics, Vol.7, No.1, pp. 1-13, 2014.
- "Human-Robot Collision Avoidance using A Modified Social Force Model with Body Pose and Face Orientation," Int. J. of Humanoid Robotics, Vol.10, Issue 1, 2013.

Membership in Academic Societies:
- The Institute of Electrical and Electronics Engineers (IEEE)
- The Robotics Society of Japan (RSJ)
- The Japan Society of Mechanical Engineers (JSME)
- The Society of Instrument and Control Engineers (SICE)
- The Institute of Electronics, Information and Communication Engineers (IEICE)
- Information Processing Society of Japan (IPSJ)
- The Virtual Reality Society of Japan (VRSJ)

Name:
Yasuhiko Arai

Affiliation:
Professor, Kansai University

Address:
3-3-35 Yamate-cho, Suita, Osaka 564-8680, Japan

Brief Biographical History:
1988 Received Ph.D. degree in Mechanical Engineering from Osaka University
2000- Professor, Mechanical Engineering Department, Kansai University

Main Works:
- "Three-dimensional shape measurement beyond the diffraction limit of lens using speckle interferometry," J. Modern Optics, doi: 1080/09500340.2018.1470266, 2018.

Membership in Academic Societies:
- The International Society for Optics and Photonics (SPIE)
- The Japan Society of Applied Physics (JSAP)
- The Japan Society for Precision Engineering (JSPE)
- The Japan Society of Mechanical Engineers (JSME)
- The Society of Instrument and Control Engineers (SICE)

Name:
Seiji Aoyagi

Affiliation:
Professor, Faculty of Engineering, Kansai University

Address:
3-3-35 Yamate-cho, Suita, Osaka 564-8680, Japan

Brief Biographical History:
1988- Research Associate, Mechanical System Engineering Department, Kanazawa University
1996- Associate Professor, Systems Management Engineering Department, Kansai University
2007- Professor, Mechanical Engineering Department, Kansai University

Main Works:
- "Proposal of Realizing Method of STS Control Based on Trajectory Planning and Trajectory Update and Experimental Verification of Its Effectiveness by Employing an Open Architecture Robot," J. of the Robotics Society of Japan, Vol.19, No.1, pp. 131-141, 2001.

Membership in Academic Societies:
- The Japan Society of Mechanical Engineers (JSME)
- The Robotics Society of Japan (RSJ)
- The Japan Society for Precision Engineering (JSPE)